

## The central oscillatory network of essential tremor

Muthuraman Muthuraman, U. Heute, Günther Deuschl, Jan Raethjen

### Angaben zur Veröffentlichung / Publication details:

Muthuraman, Muthuraman, U. Heute, Günther Deuschl, and Jan Raethjen. 2010. "The central oscillatory network of essential tremor." In 2010 Annual International Conference of the IEEE Engineering in Medicine and Biology, 31 August - 04 September 2010, Buenos Aires, Argentina, edited by Ricardo Armentano, Donna Hudson, and Emilio Sacristan, 154-57. Piscataway, NJ: IEEE. <https://doi.org/10.1109/iembs.2010.5627211>.

### Nutzungsbedingungen / Terms of use:

licgercopyright

Dieses Dokument wird unter folgenden Bedingungen zur Verfügung gestellt: / This document is made available under these conditions:

**Deutsches Urheberrecht**

Weitere Informationen finden Sie unter: / For more information see:

<https://www.uni-augsburg.de/de/organisation/bibliothek/publizieren-zitieren-archivieren/publiz/>



# The Central Oscillatory Network of Essential Tremor

Muthuraman M, Heute U, Deuschl G, and Raethjen J

**Abstract**—The responsible pathological mechanisms of essential tremor are not yet clear. In order to understand the mechanisms of the central network its sources need to be found. The cortical sources of both the basic and first “harmonic” frequency of essential tremor are addressed in this paper. The power and coherence were estimated using the multitaper method for EEG and EMG data from 6 essential tremor patients. The Dynamic Imaging of Coherent Sources (DICS) was used to find the coherent sources in the brain. Before hand this method was validated for the application of finding multiple sources for the same oscillation in the brain by using two model simulations which indicated the accuracy of the method. In all the essential tremor patients the corticomuscular coherence was also present in the basic and the first harmonic frequency of the tremor. The source for the basic frequency and the first harmonic frequency was in the region of primary sensory motor cortex, prefrontal and in the diencephalon on the contralateral side for all the patients. Thus the generation of these two oscillations involves the same cortical areas and indicates the oscillation at double the tremor frequency is a harmonic of the basic tremor frequency.

## I. INTRODUCTION

Essential tremor is commonly hereditary, and pathoanatomical studies have not yet identified any morphological changes which strongly supports the idea that this tremor is due to a structural abnormality in the central nervous system [1]. The most accepted hypotheses are the involvement of olivary nucleus and cerebellum in the tremor generation [2, 3]. However, the functional imaging [4] and deep brain stimulation studies [5, 6] indicate that the primary motor area and the thalamus are involved in tremor generation. This tremor occurs while doing voluntary actions and remains constant till the action is performed, it usually disappears at rest. The frequency of this tremor is between 4 and 9 Hz. In the present paper we use dynamic imaging of coherent sources (DICS) which applies a spatial filter to localize brain activity that is coherent with a peripheral tremor signal [7]. It has earlier been applied on MEG recordings in essential tremor [8]. However the source

analysis was applied to find the primary source and then was continued without the peripheral electromyogram (EMG) signal. In this study, we look for the sources of the basic frequency and double the tremor frequency separately by applying DICS and having the EMG as reference signal in all runs of the source analysis. The results were validated by a model simulation.

## II. METHODS

### A. Source Analysis

In order to locate the origin of a specific EEG activity seen on the scalp, two problems need to be solved which are the forward and inverse problem. The forward problem as shown in Fig. 1 is the computation of the scalp potentials for a set of neural current sources. It is usually solved by estimating the so-called lead-field matrix with specified models for the brain. In this paper, two models were used, namely, the single-sphere model in which the brain is modeled by a single sphere and the more complex five-concentric-spheres model with five different spheres for each layer as shown in Fig. 1.

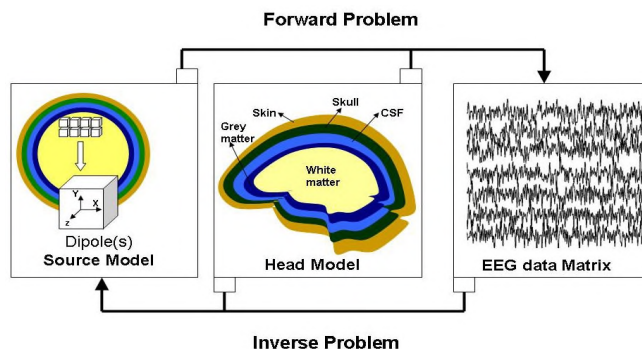


Fig. 1. EEG source analysis. The source model is defined by the different spheres with the dipole arrangement as shown with cubes called voxels. The head model shown in this figure is for the five-concentric-spheres model with the five different layers.

The **forward solution**, to determine the transmission from sources in the brain to the surface of the head where the EEG electrodes are placed, a volume conduction model is used with a boundary-element method (BEM) [9]. The head is modeled by giving in the radius and the position of the sphere with the electrode locations. In order to map the current dipoles in the human brain to the voltages on the scalp the lead-field matrix is calculated as described in [10]. The BEM allows calculating the electric potential  $\phi$  of a current source in an inhomogeneous conductor by solving the following integral equation. If the conducting object is

M. Muthuraman is with the Department of Neurology, University of Kiel, 24105 Germany. (phone: 49-431-597-8804; fax: 49-431-597-8502; e-mail: m.muthuraman@neurologie.uni-kiel.de).

Prof. U.Heute is with the Institute for Circuit and System Theory, University of Kiel, D-24143 Germany. (email:uh@tf.uni-kiel.de)

Prof. G.Deuschl is with the Department of Neurology, University of Kiel, 24105 Germany. (e-mail:g.deuschl@neurologie.uni-kiel.de)

PD. Dr. med J. H. Raethjen is with Department of Neurology, University of Kiel, 24105 Germany. (e-mail: j.raethjen@neurologie.uni-kiel.de).

divided by closed surfaces  $S_i (i = 1, 2, \dots, n_s)$  into  $n_s$  compartments, each having a different enclosed isotropic conductivity  $\sigma_j^{in}$ , the electric current due to the electric potential at position  $r \in S_k$  is then given by [11, 12]:

$$\bar{\sigma}_k \phi(r) = R + \frac{1}{4\pi} \sum_{i=1}^{n_s} \Delta\sigma_i \iint_{S_i} \sigma(r') n(r') \cdot \frac{r' - r}{|r' - r|^3} dS'_i$$

where  $R = \sigma_0 \phi_0(r)$ ; with  $\phi_0$  representing the potential of the source in an unlimited homogeneous medium with conductivity  $\sigma_0$ , the mean conductivity is  $\bar{\sigma}_k = (\sigma_k^{in} + \sigma_k^{out})/2$ , where  $\sigma_k^{out}$  is the unenclosed isotropic conductivity and the conductivity differences are given as  $\delta\sigma_i = \sigma_i^{in} - \sigma_i^{out}$ . In order to calculate the electric field, it is necessary to approximate numerically the integral over the closed surface  $S_i$  of the conductor boundaries consisting of differential surface elements ( $dS'_i$ ) and with surface normal orientations  $n$  at positions  $r'$ . The surfaces are described by a large number of small rectangles and the integrals are replaced by summations over these rectangle areas. The potential values or the coefficients of the basis functions form a vector of unknowns which is used to approximate the potentials on the surface elements, which can be solved through the following matrix formulation:

$$\bar{\sigma}\phi = \sigma_0\phi_0 + B\phi \Rightarrow \phi = (\bar{\sigma} - B)^{-1} \sigma_0\phi_0$$

If the above equation solves the first equation just for the fixed number of measurement positions, a transfer matrix  $T$  is obtained, that relates the sensor signals to the homogeneous potentials [13]. The potential vector  $\phi$ , that contains the field distribution at all skin nodes, generated by a (dipolar) source inside the innermost compartment (brain) can thus be easily computed by a simple matrix vector multiplication:

$$\phi = T\phi_0$$

with

$$T = (\sigma - B)^{-1} \sigma_0$$

The column vector  $\phi_0$  contains the electric potential values  $\phi_{0i}$  of all skin-nodes  $i$  at position  $r_i$  for the source in an infinite homogeneous conductor with conductivity  $\sigma_0$  (dipole at position  $r_j$ , current  $j$ ):

$$\phi_{0i} = \frac{1}{4\pi\sigma_0} j \frac{r_i - r_j}{|r_i - r_j|^3}$$

The BEM generalized model for  $i = 1, 2, \dots, n_s$  explained here was used for the construction of a simple single-sphere model for which the parameter  $S_i$  described in the first equation will be  $S_i = i = 1$ , and the complex five concentric-spheres-model were  $S_i = i = 5$  for the reconstruction of the sources.

The **inverse solution**, the power and coherence estimated using the Multitaper method (MTM) as described in [10], at any given location in the brain can be computed using a linear transformation which in our case is the spatial filter. The spatial filter relates the electromagnetic field on the surface to the underlying neural activity in a certain brain region. The neural activity is modeled as a current dipole or sum of current dipoles. The spatial filter, which attenuates the signals from other locations and allows only signals generated from a particular location in the brain.

The complete description of the inverse solution which uses the spatial filter is described elsewhere [10].

## B. Model Simulation

Verifying the inverse solution from real EEG data is a very difficult task because the real distribution of the current dipoles in the human brain remains unknown. Due to this, it is important to verify the method by performing simulations, which means to create a time series of current dipoles for each voxel in the data set and then calculate the corresponding EEG signal. After that, it is possible to calculate the inverse solution of these EEG signals and compare them with the generated data. In all the simulations the data was generated using the five-concentric-spheres model. The inverse solution, however was calculated with two models, namely the single-sphere and the five-concentric-spheres model, to see whether the single sphere is enough to identify the sources simulated using the more complex model. The two main aims of these simulations are to test whether simultaneously active cortical and deep sources can be detected, and to address the issue of identifying more than two sources for the same frequency of oscillation in the brain.

Detecting deep current dipole moments is a very difficult task because there are much more possibilities for the distribution of dipole sources if they are far away from the EEG electrodes and, additionally, the signals from deep neurons have to propagate through the rest of the brain tissue, which will attenuate the signal. These problems can lead to wrong inverse solutions and were therefore simulated in order to analyse their accuracy. The first idea one could have for a simulated current-dipole time series is just a dipole moment which is constant over time in some voxels. For example, one could think of a non-zero value in some voxels and a zero value in all other voxels in order to simulate a concentrated source. Using these data would be good enough for a static inverse-solution method like LORETA [14], but it is not a good model for the DICS method. The DICS assumes a dynamical process in the brain which is why the simulated data must also reflect a

dynamical process if the performance of the DICS method should be tested. Therefore we used autoregressive processes for simulating the biological situation.

In the **first simulation**, the data is generated by assuming an autoregressive (AR) process of order two defined as:

$$y(t) = a_1 y(t-1) + a_2 y(t-2) + \eta(t)$$

where  $a_1$  and  $a_2$  are the AR2 coefficients and  $\eta(t)$  is the white Gaussian noise with zero mean and unit variance, as the sources in two (active) voxels. The poles in the complex plane for the AR2 process were both 0.99, i.e.,  $a_1 = 1.979$  and  $a_2 = -0.9801$  are the AR2 coefficients for a 5Hz process. The first issue of locating the correct sources when there were two active voxels for the same frequency was taken into account.

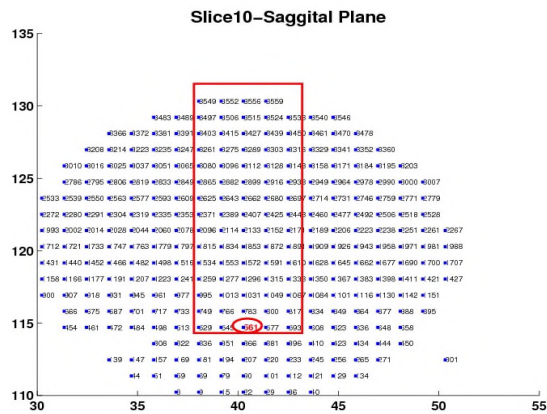


Fig. 2. The arrangements of the voxels in the slice 10 of the voxel space in the sagittal plane. The encircled red number is the chosen voxel for the step 1 in the first simulation.

In step1 the source for the 5 Hz was implemented in two active voxels, one of which was in the cortex contralateral (C) to the assumed muscle is the voxel number 3428 and the other was in the diencephalon (D) with the voxel number 561. The “EEG signal” was produced with a broad-band AR2 plus white noise of 25 % (SNR= 4 dB) (compared to the clean 5 Hz AR2 signal “of infinite SNR”) was added to the other voxels. The two active voxels were selected in such a way that they are above each other in the sagittal plane (vertical voxel plane) as shown in Fig. 2 with the same 5 Hz AR2 processess. The diencephalon source is marked in red in Fig. 2. The reference EMG signal was the 5Hz AR2 process with added broad band noise to tune the coherence to 0.5 ( as seen in real data). In order to locate two sources with the same frequency, the source analysis (DICS) needs to be repeated twice. In the first run, it locates the highest-coherent source, and this source is considered as noise for the second run of the source analysis. This is done by taking the identified voxel in the first run and assigning it into the noise normalization matrix for the next run of the source analysis. The results from the first run of the source analysis for this simulation with a single-sphere model showed a source in the midline of the cortex for the 5 Hz activity as shown in Fig. 3 A. In this simulation, the midline cortical

source (M) was not simulated. The problem has occurred because the same frequency source was simulated in two voxels which were lying vertically in the same line in the voxel plane. But, when the identified voxel is considered as noise for the second run of the source analysis, then the source analysis was able to locate the correct cortical source followed by the deep source as simulated and shown in Fig.3 A.

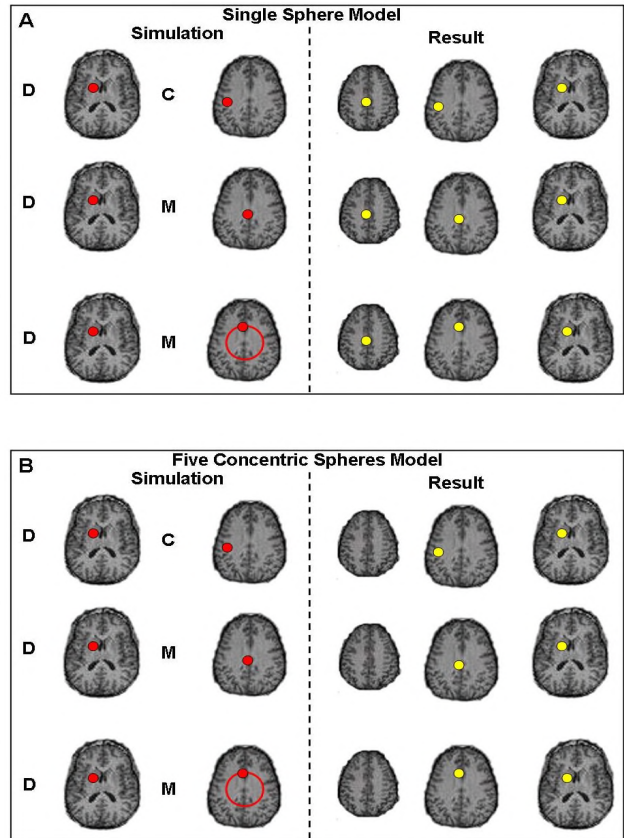


Fig.3. A. The results from a single sphere model for the first simulation. The left column slices with the red dots indicate the simulated sources. The right column slices with the yellow dots indicate the sources obtained. The active voxels were changed within the red circled area to test the algorithm with both the models. B. The results from the five concentric spheres model for the first simulation.

In order to check whether this problem occurs only in this case, the active voxels were changed within the red circled area in step2 and step3 as shown in Fig. 3 B. The conclusion was that with a single-sphere model, there could be some discrepancies in the location of the sources in two cases one of which when they are above each other in the vertical voxel plane. The second case is when they are within 3 neighbouring voxels in the sagittal plane which is marked in red with a rectangular box in Fig. 2. The problem was solved by implementing the correct concentric five spheres model which was used when simulating the data. Then, the correct location was identified for both the active voxels, even when they are above each other in the sagittal plane as shown in Fig. 3 B.

In the **second simulation**, in step1 the source for 5 Hz was implemented in three different active voxels at the contralateral motor cortex (C) with voxel number 3154, premotor cortex (PMC) with voxel number 3037 and the diencephalon (D) with voxel number 545. The source for the 10 Hz was implemented in another three different active voxels at the primary sensory motor cortex (S1) with voxel number 2948, secondary sensory motor cortex (S2) with voxel number 3222 and the posterior parietal cortex (PPC) with voxel number 2770. Both models were used to locate the sources for all the three different active voxels for both frequencies. The same problem occurred for the single sphere model as in the first simulation, but with the correct complex model all the sources were identified precisely. These two simulations show that the single sphere model may not be a good enough approximation in complex situations with multiple different sources.

### III. APPLICATION TO ESSENTIAL TREMOR PATIENTS

The DICS method was applied to 6 essential-tremor patients all of whom had clear peaks in the power spectrum, cross spectrum and coherence spectrum at the basic and first harmonic frequency. The average basic frequency for all the patients was 3.8 Hz and the average first “harmonic” frequency was 8.3 Hz.

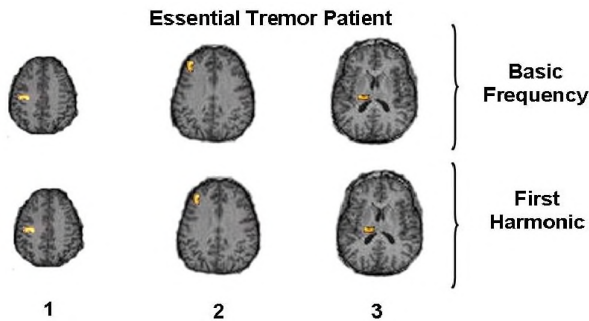


Fig. 4. The single slice plot of the basic frequency and the first harmonic frequency from the single-sphere model with all the active sources in an essential tremor patient. 1- PSMC- Primary sensory motor cortex, 2- PFC- Prefrontal cortex, 3- D- Diencephalon.

In all the patients the source for the basic frequency and the first harmonic frequency was found in the contralateral side of the brain as to be seen in the example of Fig. 4 in the slice plot with six slices of the brain. For this example patient the flexor muscle on the right was taken as the reference. In the essential tremor patients the simple single-sphere model and the five-concentric-spheres model were able to identify three sources which were involved with this tremor network. The repetitive runs of the source analysis identified the same network responsible for both the basic and first harmonic frequency of this tremor. The locations comprise the PSMC, PFC and the diencephalon as shown in Fig. 4 on single slices for each source separately. The two frequencies in these patients have almost identical origins in the brain indicating that they are likely simple harmonics and do not reflect separate oscillations as in the Parkinsonian patients [10]. The

next important result is that the deep source in ET is located more posteriorly in the diencephalon can be seen in Fig.4. This would be in keeping with the ET mainly involving the thalamus. This data clearly show that ET and the Parkinsonian tremor data from [10] originate from different central networks and could be distinguished on the basis of the source analysis.

### IV. CONCLUSION

In conclusion the model simulation showed us that with the five concentric spheres model the accuracy of the DICS is increased and leads to plausible results. The method was also able to identify correctly the multiple sources simulated for the basic and first harmonic frequencies. Thus our findings in essential tremor patients using the same method do not reflect a methodological artifact but likely indicate that the two peaks at the tremor frequency and around the double value are simply harmonics and do not reflect independent oscillations involving separate cortical sources as in the Parkinson’s disease [10].

### ACKNOWLEDGMENT

Support from the German Research Council (Deutsche Forschungsgemeinschaft, DFG, SFB 855, Project D2) is gratefully acknowledged.

### REFERENCES

- [1] G. Deuschl, J. Raethjen, M. Lindemann, P. Krack, “The pathophysiology of Parkinsonian tremor”, *Muscle Nerve* 24, 2001, pp. 716-735.
- [2] D. Lorenz, G. Deuschl, “Update on pathogenesis and treatment of essential tremor”, *Curr. Opin. Neurol*, 20, 2007, pp. 447-452.
- [3] E. D. Louis, J. P. Vonsattel, “The emerging neuropathology of essential tremor”, *Mov. Disord* 23, 2008, pp.174-182.
- [4] S. F. Bucher, “Activation mapping in essential tremor with fMRI”, *Ann. Neurol.* 41, 1997, pp.32-40.
- [5] K. E. Lyons, R. Pahwa, “Deep brain stimulation and essential tremor”, *J. Clin. Neurophysiol* 21, 2004, pp. 2-5.
- [6] J. P. Hubble, K. L. Busenbark, S. Wilkinson, R. D. Penn, K. Lyons, W. C. Koller, “Deep brain stimulation for essential tremor”, *Neurology* 46, 1996, 1150-1153.
- [7] J. Gross, “Dynamic imaging of coherent sources: Studying neural interactions in the human brain” *PNAS* 98, 2001, pp.694-699.
- [8] A. Schnitzler, C. Munks, M. Butz, L. Timmermann, J. Gross, “Studying brain network associated with essential tremor as revealed by magnetoencephalography”, *Mov. Disord.* 24 (11), 2009, pp.1629-1635.
- [9] M. Fuchs, J. Kastner, M. Wagner, S. Hawes, J. S. Ebersole, “A standardized boundary element method volume conductor model”, *Clinical Neurophysiology* 113 (5), 2002, pp.702-712.
- [10] M. Muthuraman, J. Raethjen, H. Hellriegel, G. Deuschl, U. Heute, “Imaging coherent sources of tremor related EEG activity in patients with Parkinson’s disease”, *IEEE EMBC*, 2008, 113 (5), pp.4716-4719.
- [11] D.B. Geselowitz, “On bioelectric potentials in an homogeneous colume conductor”, *Biophysical Journal*, 1967, pp.165-171.
- [12] J. Sarvas, “Basic mathematical and electromagnetic concepts of the biomagnetic problem”, *Phy. Med. Biol.* 32, 1987, pp.11-22.
- [13] D.J. Fletcher, “Improved method for computation of potentials in a realistic head shape model”, *IEEE Trans. Biomed. Eng.* 42, 1995, pp. 1094-1104.
- [14] R.D. Pascual-Marqui, “Low resolution electromagnetic tomography: a new method for localizing electrical activity in the brain”, *Int. J. of Psychophysiol.* 18, 1994, pp. 49-65.